J. Phys. E: Sci. Instrum., Vol. 18, 1985. Printed in Great Britain

A method for determining electron mobility and attachment to molecular impurities in high density gases†

L Bruschi, M Santini and G Torzo
Dipartimento di Fisica dell'Università di Padova and
Gruppo Nazionale Struttura della Materia, Padova, Italy

Received 15 June 1984, in final form 19 August 1984

Abstract. We report here a detailed description of a new technique used for the measurement of the mobility of electrons in dense gases and their attachment frequency to molecular impurities. The effect of space charge, that can be relevant in the 'zero field mobility' measurement, is evaluated.

1. Introduction

When thermalised electrons injected into high density gases are captured by molecular impurities, the electron density n_e decreases according to the exponential law

$$n_e(t) = n_e(0) \exp(-t/\tau) \tag{1}$$

where τ is the mean life of the injected electrons, and $\nu_A = (1/\tau)$ is the attachment frequency. If a slice of such electrons drifts with velocity v_e, the density at a distance $x = v_e t$ from the injector is

$$n_e(x) = n_0 \exp(-x/\lambda) \tag{2}$$

where λ is the attenuation length and $n_0 = n_e(0)$.

It has been observed that in a dense gas the role of the impurities becomes important even at a very low concentration, lower than 10^{-6}. In extreme situations the electron swarm can be completely attenuated over a distance smaller than the experimental drift distance, thus inhibiting any measurements on free electrons. In a less dramatic situation, the slow molecular ions produced by electron attachment can build up a relevant space charge electric field that seriously distorts the applied electric field. To minimise these effects one must reduce drastically both the impurity content and the electronic current used in the measurements.

We describe in this paper a technique recently developed in our laboratory which allows simultaneous measurements of the electron mobility and of the attachment frequency.

The essential features of our method have been described briefly in our previous papers. Here we present more details of the calculations and of the experimental apparatus.

2. The method of measurement

2.1. Experimental set-up

Four plane and parallel electrodes are immersed in the fluid to be studied (figure 1). S is a radioactive source that ionises a thin fluid layer, and is kept at a negative potential V_s with respect to the first grid G_1. G_1 acts as a steady emitter of both thermalised electrons and negative ions, and the intensity of the emitted current is controlled by V_s. G_1 is driven, with respect to the second grid G_2, by an unbalanced square wave V_1 at a constant frequency $f_1 = (2T_1)^{-1}$, of amplitude V_1^- in the forward half period and V_1^+ in the reverse one. Because the ion mobility is much lower than the electron mobility ($\mu_e/\mu_i \simeq 10^3$), the half period T_1 can be chosen to be longer than the electronic transit time across the G_1G_2 region, but shorter than the ionic one. Thus ions coming from the SG_1 region cannot reach G_2, and only electrons are injected into the drift region G_2C. If T_1 is chosen to be very small with respect to the ion transit time across G_1G_2, almost no ions produced within G_1G_2 can reach G_2 (see relation (12)). Because $V_1^+ > V_1^-$ these ions are swept back to G_1, and only the ions generated close to G_2 can pass through. This residual ion current entering into the drift space can be made negligible, as shown by the calculations developed in the following. Therefore we can take account only of the ions generated in the drift space G_2C.

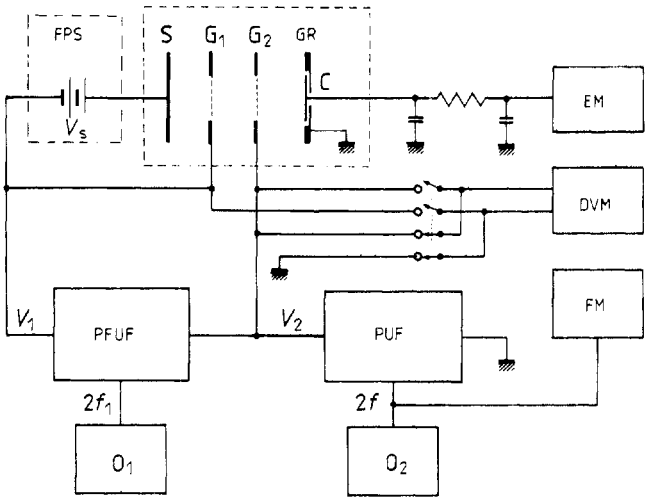

Figure 1. Schematic diagram of the measuring apparatus. S, radioactive source; G_1 and G_2, grids; C, collector; GR, guard ring; EM, electrometer; FM, frequency meter; DVM, digital voltmeter; O_1 and O_2, oscillators; FPS, floating power supply; PFUF and PUF, presettable flipflops.

The second grid G_2 is also driven, with respect to the collector C, by an unbalanced square wave V_2 of frequency $f = (2T)^{-1}$, of amplitude V_2^- in the forward half period T, and V_2^+ in the reverse one, with $V_2^+ > V_2^-$. The mean current $\bar{i}$ at the collector C is measured as a function of the frequency f.

Let us suppose now that there is no electron attachment, i.e. $\nu_A = 0$. In this case the mean collected current is given by

$$\begin{aligned} \bar{i} &= (I_0/2)(1 - f/f_e) && \text{for } f \leqslant f_e \\ \bar{i} &= 0 && \text{for } f \geqslant f_e \end{aligned} \tag{3}$$

where $f_e = (2\tau_e)^{-1}$, τ_e is the electron time of flight, and I_0 is the injected current at G_2, which can be measured by driving G_2 by a DC voltage $V_0 \equiv V_2^-$. From the measurement of the cut-off frequency f_e of the applied potential V_2^-, and of the drift distance d between G_2 and C, we obtain the electron mobility $\mu_e = 2d^2 f_e / V_2^-$.

When $\nu_A \neq 0$ the relations (3) are no longer valid. Let us suppose that the ion production is at such a low level that space charge effects can be neglected.

† Work sponsored by Consiglio Nazionale delle Ricerche and Ministero Pubblica Istruzione, Roma, Italy.

0022-3735/85/030239 + 05 $02.25

If the collector has unit area, the electronic and ionic charges, Q_e and Q_i, collected in the forward half period are given by

$$Q_e = e\int_0^T v_e n_e(t)\,dt, \qquad Q_i = e\int_0^T v_i n_i(t)\,dt \tag{4}$$

where v_e and v_i are the electron and ion drift velocities, n_e and n_i are the electron and ion number densities at the collector, and e is the electron charge. In the following reverse half period no charges are collected and therefore the total mean current is given by

$$\bar{i} = (Q_e + Q_i)/(2T). \tag{5}$$

2.2. The electron current

In our planar geometry let the grid G_1, placed at $x=0$, start injecting electrons at the beginning of the forward half period ($t=0$), with a current per unit area $I_0 = ev_e n_0$. At the collector ($x=d$) there are no electrons until $t=\tau_e$. At $t=T$ the electric field is reversed. The electron density at G is therefore $n_e=0$ for $0\leqslant t\leqslant\tau_e$, $n_e = n_0\exp(-d/\lambda)$ for $\tau_e\leqslant t\leqslant T$ and $n_e=0$ for $T\leqslant t\leqslant 2T$. From (4) we get the electronic charge collected in one period, $Q_e = I_0\exp(-d/\lambda)(T-\tau_e)$, and the electronic current may be written as

$$\bar{i}_e = (I_0/2)\exp(-r)(1-f/f_e) = I^*(1-f/f_e) \tag{6}$$

where

$$r = d/\lambda = \nu_A/(2f_e), \qquad I^* = (I_0/2)\exp(-\nu_A/2f_e).$$

2.3. The ionic current

Let us consider a thin slice of neutral impurities that are at x_0 at the beginning of the forward half period. The first electrons reach them at time $t_0 = x_0/v_e$. At this time the attachment process produces the first ions, which start drifting towards the collector with velocity v_i. They reach the collector at time t given by $d = x_0 + v_i(t-t_0)$.

A slice of ions reaching the collector at the time t therefore originates at a point x_0 given by

$$x_0 = (d - v_i t)v_e/(v_i - v_e) \tag{7}$$

and was at x' at the time t', with $x' = x_0 + v_i(t'-t_0)$. At x' more ions are produced which start drifting. The density of the ion slice thus increases according to the enrichment law

$$dn_i = \nu_A n_0\exp(-x'/\lambda)\,dt' = \nu_A n_0\exp(-x'/\lambda)(dx'/v_i). \tag{8}$$

The final density is given by

$$n_i(d,t) = (\nu_A n_0/v_i)\int_{x_0}^{d}\exp(-x'/\lambda)\,dx'.$$

One obtains after some rearrangement

$$n_i(d,t) = n_0\alpha\exp(-r)\exp\left[\left(r\frac{t-\tau_e}{\tau_i-\tau_e}\right)-1\right], \tag{9}$$

where $\alpha = v_e/v_i$ and $\tau_i = d/v_i$.

The relation (8) is valid for $\tau_e\leqslant t\leqslant\tau_i$. For $t\leqslant\tau_e$, $n_i=0$ because no electrons have reached the collector. For $\tau_e\leqslant t\leqslant\tau_i$, n_i increases with time, according to relation (9), from zero up to the steady value n_{is}. At $t=\tau_i$ we are dealing in fact with the slice born at the grid $G_2(x_0=0)$, and we reach the stationary situation, where n_{is} is given by

$$n_{is} = n_0\alpha[1-\exp(-r)], \tag{10}$$

obtained from (9) for $t=\tau_i$.

To obtain from (9) and (10) the collected ionic charge Q_i, we must distinguish two different frequency ranges: $0\leqslant f\leqslant(2\tau_i)^{-1}$ and $(2\tau_i)^{-1}\leqslant f\leqslant(2\tau_e)^{-1}$.

2.4. The low frequency range

When the half period T is greater than the ionic transit time τ_i, in the cleaning half period all the ions have time enough to reach the grid G_2. At the beginning of the forward half period the drift space is clean. The relation (4) becomes

$$Q_i = ev_i\left(\int_{\tau_e}^{\tau_i} n_i(d,t)\,dt + \int_{\tau_i}^{T} n_{is}\,dt\right),$$

and using (5), (9) and (10) one obtains the mean current $\bar{i}$

$$\bar{i} = (I_0/2)(1-Kf/f_i), \qquad 0\leqslant f\leqslant f_i, \tag{11}$$

where $f_i = (2\tau_i)^{-1}$ and $K = 1-(1-\tau_e/\tau_i)[1-\exp(-r)]/r$. The current is a linear function of f, with a value $(I_0/2)$ at $f=0$. At $f=f_i$ it is still different from zero.

2.5. The high frequency range

Most of the ions not collected in the forward half period cannot reach G_2 in the next reverse half period, because $T<\tau_i$. In the following half period they will move again towards the collector, without reaching it, however. They are trapped betweeen G_2 and C. To remove them we use the trick of applying a reverse field higher than the forward field. In this way they move back, as a mean, and after some periods they meet the grid. We can forget them, accounting only for the ions collected in the forward half period that we are analysing. In the high frequency range we have therefore

$$Q_T = Q_e + ev_i\int_{\tau_e}^{T} n_i(d,t)\,dt,$$

and the mean current becomes

$$\bar{i} = (I_0/2)\exp(-r)(1-f/f_e)G(z) = \bar{i}_e G(z) \tag{12}$$

where

$$G(z) = \frac{[\exp(z)-1]}{z}, \qquad z = (\nu_A/2)\left(\frac{1}{f}-\frac{1}{f_e}\right)\Big/(\alpha-1).$$

The relation (12) is valid for $f_i\leqslant f\leqslant f_e$. For $f\geqslant f_e$ obviously $\bar{i}=0$. The function $G(z)$ measures the departure of relation (12) from the linear law (6). For small z, $G(z)\cong 1$, which means that the ionic contribution to the total current $\bar{i}$ is negligible. The higher the frequency, the better is the approximation of the total current $\bar{i}$ to the electronic current $\bar{i}_e$. For a plot of the mean current $\bar{i}(f)$, see Bruschi *et al* (1984a). If we want $G(z)$ to be smaller than $(1+\varepsilon)$, we must operate at frequencies $f>f_\varepsilon$, where

$$f_\varepsilon = f_e\left(1+\frac{4f_e}{\nu_A}(\alpha-1)\varepsilon\right)^{-1}. \tag{13}$$

In this frequency range, and within this approximation, we can use the linear relation (6) as interpolation of the experimental data.

2.6. The measurement of μ_e and ν_A

Extrapolating the linear relation to zero current we obtain f_e, and so the mobility:

$$\mu_e = 2d^2 f_e/V_2^-. \tag{14}$$

Extrapolating to zero frequency we obtain the value of $I^* = (I_0/2)\exp(-\nu_A/2f_e)$ which is the electronic contribution, at $f=0$, to the total collected current. From this value and from the value of I_0 (i.e. the current measured applying to G_2 a constant potential $V_0 \equiv V_2^-$) we obtain the value of the attachment frequency

$$\nu_A = 2f_e\ln(I_0/2I^*). \tag{15}$$

A simultaneous measurement of electron mobility and of

attachment frequency to molecular impurity is therefore possible in the same experimental cell and with the same sample gas.

The previous discussion can be identically repeated also for the G_1G_2 region. The relation (12) therefore can be used to choose values for f_1 and V_1^- that make negligible the ionic current injected through G_2.

3. Space charge effects

3.1. Electronic and ionic contribution

The previous analysis has been performed neglecting any space charge effects. The electronic contribution to the space charge is usually negligible. Suppose in fact that we are dealing with a pure electronic current of density I_0. If the space charge electric field E' is small with respect to the applied electric field E, we can assume the charge density to be constant over the whole drift space. The absolute value of E' at the grid and at the collector is then $|E'| = I_0 d/(2\varepsilon_0 v_e)$, where ε_0 is the vacuum permittivity. With $I_0 = 10$ pA cm^{-2}, $d = 0.5$ cm, $v_e = 50$ m s^{-1}, we get $E' = 5 \times 10^{-3}$ V cm^{-1}.

If the same current density I_0, on the contrary, is a pure ionic current, with $v_i \cong 10^{-3} v_e$ we get $E' \cong 5$ V cm^{-1}.

The situation is thus difficult when we are measuring the electron mobility, because μ_e becomes field independent only at small electric fields. At high gas densities, $N = (1-10) \times 10^{21}$ cm^{-3}, even a very low impurity concentration ($C < 10^{-6}$) causes a relevant attenuation of the electron swarm (Bruschi *et al* 1984a, b). Because of their low mobility, the ions accumulate in the drift space and the space electric field E' becomes easily of the same order of magnitude as the small applied electric field E. To avoid this situation both the impurity concentration and the injected current I_0 must be kept as small as possible.

A complete discussion of the space charge problem is difficult. We will here examine the situation where the space charge electric field is small with respect to E. In this situation we can assume the electron and ion drift velocities to be constant over the whole drift space. The electronic space charge will also be neglected, and we will only calculate the effect due to the ion charge density

$$\rho_i(x) = e n_i(x). \tag{16}$$

3.2. The DC case

Let us first consider the case of a constant electric field $E = V_0/d$ applied to the drift space, with $V_0 \equiv V_2^-$. In this steady situation the ion density $n_i(x)$ is obtained by integrating between 0 and x the enrichment law (8): $n_i(x) = n_0 \alpha [1 - \exp(-x/\lambda)]$. The electric field E' produced at the grid G_2 by this distribution can be easily calculated with the aid of the Gauss theorem:

$$\frac{E'}{E} = 5.6 \times 10^{12} \left(\frac{I_0 d}{\mu_i E^2}\right)\left(\frac{1-\exp(-r)}{r} - 1\right) \tag{17}$$

where E', E are measured in V cm^{-1}, I_0 in A cm^{-2}, μ_i in cm^2 V^{-1} s^{-1}, and d in cm. E' can be reduced by decreasing ν_A, i.e. the impurity concentration, or by increasing E. If the impurity content cannot be made small enough, or if we need impurities to study the attachment process, then the current density I_0 must be reduced to small values.

3.3. The AC case

Suppose now we are measuring the mobility μ_e with the square wave V_2 applied to G_2. If $E_- = V_2^-/d$ is the applied electric field and $E'(x)$ is the space charge field, then the measured electron time of flight τ_e' is given by

$$\tau_e' = (1/\mu_e) \int_0^d [E + E'(x)]^{-1} \, dx.$$

In the situation of interest ($E'(x) \ll E$) we easily obtain $\tau_e' \simeq \tau_e(1 - \bar{E}'/E)$, where τ_e is the value one would measure with $E' = 0$, and where $\bar{E}' = d^{-1} \int_0^d E'(x)\, dx$ is the spatial average of $E'(x)$. The relative error is then

$$\Delta = (\mu_e' - \mu_e)/\mu_e = -(\tau_e' - \tau_e)/\tau_e = \bar{E}'/E.$$

A simple way to calculate $n_i(x)$ in the case $E' \ll E$ and $v_i \ll v_e$ is the following. Because $V_2^+ > V_2^-$, we think of the ions as drifting, on average, toward G_2 with a mean velocity $v_i^* = \mu_i(E_+ - E_-)/2 = \mu_i E_-(\beta - 1)/2$, where $\beta = (E_+/E_-)$. Because electrons are injected only during the forward half period, the effective injected density is now $n_0^* = n_0/2$. Using the relation (8), with the position $dt' = -(dx'/v_i^*)$ we get

$$n_i(x) = (\nu_a n_0^*/v_i^*) \int_d^x \exp(-x'/\lambda)\, dx'.$$

This space charge distribution produces an electric field $E'(x)$ that can be written as

$$E'(x)/E_- = 5.6 \times 10^{12} (I_0 d/\mu_i E_-^2)(\beta - 1)^{-1} f(x, r) \tag{18}$$

where

$$f(x, r) = \left(\frac{1}{r} + 1\right) \exp(-r) + \frac{1}{r} - 2\left(\frac{x}{d}\right) \exp(-r) - \left(\frac{2}{r}\right) \exp\left(-\frac{x}{\lambda}\right).$$

For the order of magnitude of $|E'(0)/E_-|$ at the grid G_2, we can repeat what was observed for the DC case, with the difference that in the AC case we can make $v_i^* \gg v_i$ by increasing the reverse field, that is β. After averaging $E'(x)$ over the drift space we get for the relative error $\Delta\mu/\mu$

$$\Delta\mu/\mu = 5.6 \times 10^{12} (I_0 d/\mu_i E_-^2)(\beta - 1)^{-1} g(r) \tag{19}$$

where

$$g(r) = \left(\frac{1}{r}\right)\left[\left(1 + \frac{2}{r}\right) \exp(-r) - \left(\frac{2}{r}\right) + 1\right], \qquad g(r) < 0.14.$$

The relative error depends on many parameters. It is small at high fields, not only because of the factor E_-^2, but also because at high fields we have larger v_e and therefore small r. Moreover the error can be reduced by increasing $\beta = V_2^+/V_2^-$. As an example with $\beta = 10$, $E_- = 1$ V cm^{-1}, $I_0 = 10^{-12}$ A cm^{-2}, $\mu_i = 1$ cm^2 V^{-1} s^{-1} and $r = 1$, we get $\Delta\mu/\mu \simeq 3\%$. In general relation (19) enables us to choose the experimental parameters I_0, β and $r = d\nu_a/v_e$ to meet the desired accuracy for each value of the applied electric field E.

4. Experimental details and results

The experimental apparatus has been described briefly elsewhere (Bruschi *et al* 1984a). Here we report only the details not previously published and some improvements introduced in the circuitry and in the gas handling system.

A block diagram of the circuitry is shown in figure 1. The interelectrode separations are $d_{SG_1} = 13$ mm, $d_{G_1G_2} = 2$ mm and $d_{G_2C} = 5$ mm.

The adjustable potential difference V_s is produced by a floating power supply FPS. The square wave V_1 is produced by a homemade presettable floating unbalanced flipflop, PFUF, driven by an internal oscillator O_1 of frequency $2f_1$. Both FPS and PFUF are specially designed to have a small capacity with respect to the common ground (figure 2). The square wave V_2 is produced by a similar presettable unbalanced flipflop PUF, driven by an external oscillator O_2 of frequency $2f$. Both PFUF and PUF can either run in the clock mode triggered by O_1 and O_2, to get the unbalanced square waves, or be blocked on the high or low state, through a switch SW, to get positive or negative constant potential differences. The amplitudes V_1^+, V_1^-, V_2^+ and V_2^- can be independently adjusted.

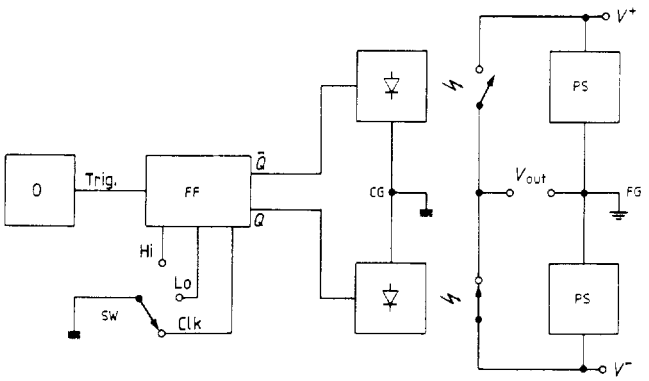

Figure 2. Block diagram of the presettable floating unbalanced flipflop PFUF. O, driving oscillator; FF, presettable flipflop; CG, common ground; FG, floating ground. PS are power supplies with low capacity with respect to CG. The floating output stage is a double electronic switch, driven by FF via a DC optical coupling.

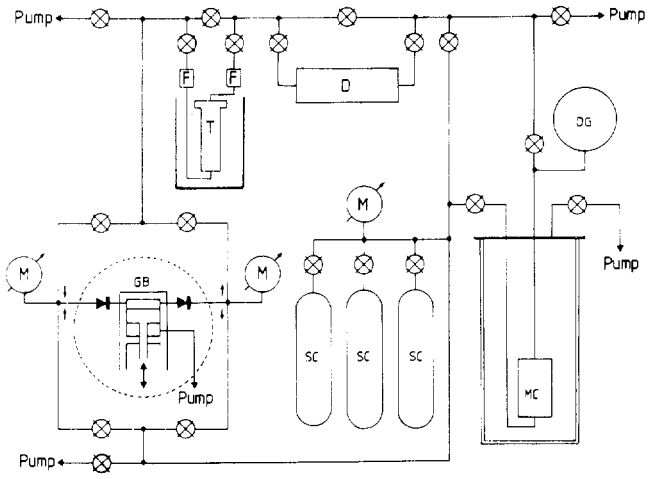

Figure 3. Schematic diagram of the gas handling system. GB, gas booster; F, sintered metal filter; T, LN_2 cooled charcoal trap; D, deoxidiser; DG, digigauge; M, manometer; MC, measuring cell; SC, storage cylinder.

A schematic diagram of the improved recirculating purification plant is shown in figure 3. The sample gas, supplied by high pressure cylinders SC, flows into the measuring cell through a cold charcoal trap T and a deoxidising unit D (Oxisorb, Meissner Griesheim Gmb). The trap is provided with suitable filters F to prevent dust contamination.

The gas can be forced to circulate at the working pressure in a closed loop including T, D and the measuring cell, by means of an oil-free compressor unit (Haskel AG15 Gas Booster). The sealing between the piston head and the cylinder housing wall is provided by a modified PTFE gasket assembly. The piston is driven by compressed air. To avoid possible gas contamination, both the back volume (BV), swept by the piston head, and the small chamber separating BV from high pressure air are kept pumped. The direction of the flow in the gas loop can be reversed so that all the gas can be recovered and compressed into the storage cylinders. The low pressure Oxisorb cartridge is inserted into a high pressure container which can be evacuated before breaking the cartridge sealings.

In figure 4 we show the behaviour of our pulsed injecting method. The grid G_2 was kept at $V_0 \equiv -20$ V, while G_1 was driven by a square wave V_1 at the frequency $f_2 = 2$ kHz. We changed the reverse voltage V_1^+ from $V_1^+ = 44$ V down to zero value, while the forward voltage V_1^- was kept constant ($V_1^- = -3.8$ V). As shown in the figure, the mean current injected in the drift space was constant down to $V_1^+ \simeq 5$ V.

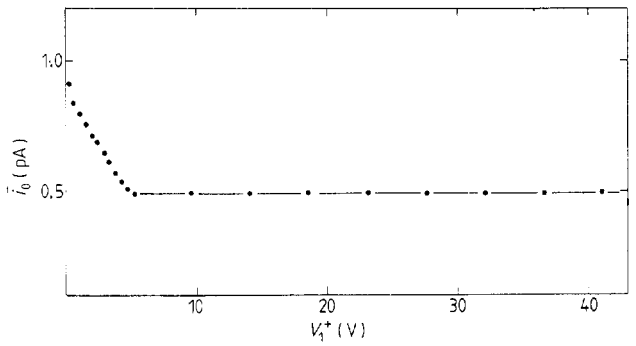

Figure 4. The current $\bar{i}_0$ measured at the collector for different values of the potential V_1^+. We used neon with $T = 293$ K, $P = 13$ Atm, $\nu_A = 16$ kHz. $V_s = -200$ V, $V_2 = -20$ V, $V_1^- = -3.8$ V.

Below this value the current increases because the reverse field E_1^+ is not strong enough to prevent spurious injection of ions by diffusion or by space charge effects. This result indicates that an unbalanced injecting square wave is needed when impurities are present, as explained in preceding sections. This particular check was made in neon at room temperature, $P = 13$ Atm, and $\nu_A \simeq 16$ kHz.

The attachment frequency ν_A should depend only on the temperature, density, and impurity content of the gas investigated. If we change the applied electric field, we change v_e, and therefore $\lambda = (v_e/\nu_A)$ and the attenuation of the electronic swarm. But ν_A should turn out independent of the electric field. Some measurements of ν_A in neon at $T = 86$ K, $N = 5 \times 10^{21}$ cm^{-3} are reported in figure 5, to show the correct behaviour of the method of measurement. Another check has been reported in Bruschi *et al* (1984a), where we showed that the measured ν_A depends linearly on the oxygen concentration. The absolute values of ν_A were moreover in excellent agreement with those found by Bartels (1973) in the same physical situation.

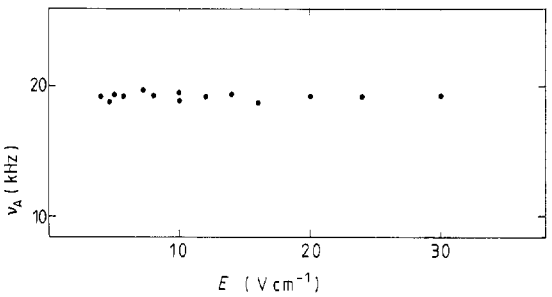

Figure 5. The measured attachment frequency ν_A plotted against the applied electric field $E = V_2^-/d$, in neon at $T = 86$ K, $N = 5 \times 10^{21}$ cm^{-3}.

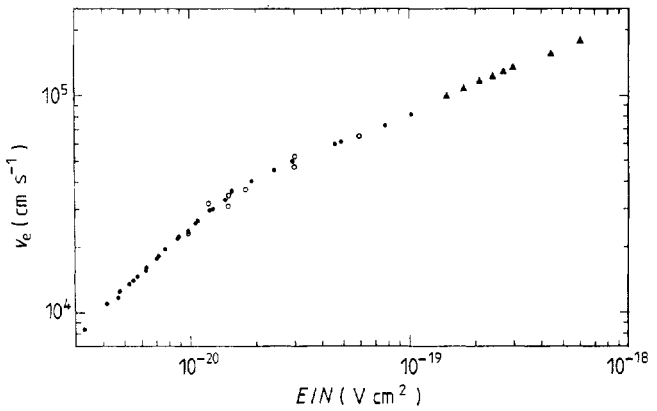

Figure 6. The measured electronic drift velocity v_e plotted against the reduced electric field E/N, where N is the gas number density. Full circles: data obtained with the present technique. Triangles: Robertson (1974). Open circles: Pack and Phelps (1961). We used neon at $T = 293$ K.

In figure 6 we report new results on the electron drift velocity as a function of E/N obtained in neon gas at room temperature, compared with those obtained by Robertson (1972) and Pack and Phelps (1961). The agreement with existing data at high E/N is good. The region of low E/N values where the electronic mobility becomes field independent has been reached for the first time by the present technique (Bruschi *et al* 1984b).

References

Bartels A 1973 Density dependence of the electron attachment frequency in dense helium-oxygen mixtures
Phys. Lett. **45A** 491–2

Bruschi L, Santini M and Torzo G 1984a Resonant electron attachment to oxygen molecules in dense helium-gas
J. Phys. B: At. Mol. Phys. **17** 1137–54

Bruschi L, Santini M and Torzo G 1984b Electron mobility in high density neon gas
Phys. Lett. **102A** 102–5

Pack J I and Phelps A V 1961 Drift velocity of slow electrons in He, Ne, Ar, H_2 and N_2
Phys. Rev. **121** 798–806

Robertson A G 1972 The momentum transfer cross section for low energy electrons in neon
J. Phys. B: At. Mol. Phys. **5** 648–64